Haplotype Associated RNA Expression (HARE) Improves Prediction of Complex Traits in Maize

Anju Giri[1*], Merritt Khaipho-Burch[2], Edward S. Buckler[1,2,3] , Guillaume P. Ramstein[1,#a*]

[1]Institute of Genomic Diversity, Cornell University, Ithaca, NY, 14853

[2]Plant Breeding and Genetics Section, Cornell University, Ithaca, NY, 14853

[3]U.S. Department of Agriculture-Agricultural Research Service, Ithaca, NY, 14853

[#a]Current Address: Center for Quantitative Genetics and Genomics, Aarhus University, Aarhus, Denmark, 8000

[*]Corresponding author

E-mail: ag2484@cornell.edu (AG), ramstein@qgg.au.dk (GPR)

Abstract

Genomic prediction typically relies on associations between single-site polymorphisms and traits of interest. This representation of genomic variability has been successful for prediction within populations. However, it usually cannot capture the complex effects due to combination of alleles in haplotypes. Therefore, accuracy across populations has usually been low. Here we present a novel and cost-effective method for imputing *cis* haplotype associated RNA expression (HARE, RNA expression of genes by haplotype), studied their transferability across tissues, and evaluated genomic prediction models within and across populations. HARE focuses on tightly linked *cis* acting causal variants in the immediate vicinity of the gene, while excluding *trans* effects from diffusion and metabolism, so it would be more transferrable across different tissues and populations. We showed that HARE estimates captured one-third of the variation in gene expression and were more transferable across diverse tissues than the measured transcript expression. HARE estimates were used in genomic prediction models evaluated within and across two diverse maize panels – a diverse association panel (Goodman Association panel) and a large half-sib panel (Nested Association Mapping panel) – for predicting 26 complex traits. HARE resulted in up to 15% higher prediction accuracy than control approaches that preserved haplotype structure, suggesting that HARE carried functional information in addition to information about haplotype structure. The largest increase was observed when the model was trained in the Nested Association Mapping panel and tested in the Goodman Association panel. Additionally, HARE yielded higher within-population prediction accuracy as compared to measured expression values. The accuracy achieved by measured expression was variable across tissues whereas accuracy using HARE was more stable across tissues. Therefore, imputing RNA expression of genes by haplotype is stable, cost-effective, and transferable across populations.

Keywords: haplotype, gene expression, genomic prediction, HARE, transferability

Author summary

The increasing availability of genomic data has been widely used in the prediction of many traits. However, genome wide prediction has been mostly carried out within populations and without explicit modeling of RNA or protein expression. In this study, we explored the prediction of field traits within and across populations using estimated RNA expression attributable to only the DNA sequence around a gene. We showed that the estimated RNA expression was more transferable than overall measured RNA expression. We improved prediction of field traits up to 15% using estimated gene expression as compared to observed expression or gene sequence alone. Overall, these findings indicate that structural and functional information in the gene sequence are highly transferable.

53 **Introduction**

54 Genomic prediction is a powerful tool to predict quantitative traits using genomic information. In
55 genomic prediction models, genome-wide predictors are simultaneously incorporated in the
56 model in an attempt to capture variation from all quantitative trait loci (QTL) associated with the
57 quantitative trait [1]. Genome-wide predictors could be single nucleotide polymorphisms (SNPs),
58 haplotypes, or any downstream intermediate responses such as transcriptomes or metabolomes
59 [1–6]. Haplotype sometimes yield higher prediction accuracy when compared to SNPs as they
60 can capture local epistatic effects, can be in tight linkage with the QTL, and can better capture
61 ancestral (identity by descent) relationships [7–10]. Haplotype-based models may be more useful
62 as beneficial haplotypes are conserved across generations due to tight linkage. Downstream
63 responses like gene expression may be biologically "closer" to the phenotype as they reflect
64 transcription processes in different tissues. However, transcription is greatly affected by tissue,
65 time, and growing conditions; therefore, transcriptome information from different tissues has
66 varying power to predict phenotypes [2,4].

67

68 Gene expression is a complex phenomenon involving interaction between DNA, cell
69 components, and the environment. Although every tissue in a plant contains the same genomic
70 sequence, gene expression varies widely across tissues producing numerous phenotypes. The
71 variation in gene expression is due to the differences in the regulatory regions and regulatory
72 genes. Discerning the role of different factors contributing to expression is a challenge; however,
73 a common approach to analyzing expression is to partition it into *cis* and *trans* components. The
74 *cis* components are polymorphisms linked to the gene, whereas the *trans* are everything else not
75 directly linked to the gene of interest [11]. *Trans* components are impacted by polymorphisms

76 arising anywhere in the genome and affect gene expression by the products from diffusion and
77 metabolism [12]. In maize like all eukaryotes, the expression of any gene is often impacted by
78 dozens of transcription factors encoded in *trans* all across the genome [13]. Therefore, *trans*
79 components frequently explain more variation in expression than *cis* components.
80
81 Different approaches exist to partition the variation in expression and infer the contribution to
82 expression by *cis* factors only. These include hybrid crosses between inbreds and different testers
83 to partition out background variation from *trans* [11,14], or analyses of genomic sequence linked
84 to genes [15]. Here, we used haplotypes in the gene region and partitioned variation in
85 expression contributed by the *cis* haplotype. Grundberg et al. [16] found that 90% of *cis* variants
86 were shared across plants growing in different environmental conditions and only a few *cis*
87 variants were environment specific as opposed to *trans* variants. The *cis* component of variation
88 is less sensitive to genetic and environmental perturbation, so, they can be stable across different
89 contexts and biological replicates. Partitioning out the variation due to *trans* from overall
90 expression allowed us to get expression effect associated with the *cis* haplotype. We called this
91 transferrable portion of the gene expression as the *cis H*aplotype Associated RNA Expression
92 (HARE). We hypothesized that HARE would be more transferable across tissues than total
93 measured transcript expression. Moreover, the consistent functional and structural information in
94 HARE would result in higher prediction accuracy than total measured expression in predicting
95 many complex traits.
96
97 We used maize to study transferability across different systems (tissues and populations) as it is
98 an important cereal crop as well as an excellent model system for quantitative genetic studies

99 [17]. Maize's genotypic and phenotypic diversity has been explored in several studies using
100 different mapping populations, uncovering thousands of genotypes and traits [18]. One example
101 is the Goodman Association panel, which represents the global diversity of inbred genotypes
102 from public maize breeding programs, including approximately 280 genotypes from tropical and
103 temperate regions, sweet corn, and popcorn lines [19]. The nested association mapping panel
104 (NAM) includes a set of approximately 5,000 recombinant inbred lines developed from 25
105 diverse inbreds crossed to a common parent, B73 [20,21]. NAM captures a large proportion of
106 diversity in maize with less confounding by population structure as would occur in an association
107 mapping panels. Both populations have been extensively genotyped and phenotyped for complex
108 traits [22–25]. In addition, the Goodman Association panel also has a large set of available
109 expression data from diverse tissues [26]. Recently these populations were used in the
110 development of a Practical Haplotype Graph (PHG) utilizing high quality assemblies of NAM
111 founder lines [27]. The PHG summarizes the diversity of these lines as a collection of haplotypes
112 in a graph [27]. In diverse species like maize, with rich allelic series, a wide range of possible
113 alleles might result in the same molecular outcome (e.g., gene expression, protein expression,
114 etc.), a process known as equifinality. HARE can parsimoniously summarize a large series of
115 allelic variants including causal variants, resulting in transferability across populations.
116 Therefore, we hypothesized that HARE would be functionally relevant beyond genomic
117 relationships and would result in higher prediction accuracy than haplotype structure when used
118 to predict many complex traits within and across populations.
119
120 To test these hypothesis, we designed a novel method for imputing expression associated with
121 haplotypes in the genic regions by HARE and studied the transferability of imputed expression

across tissues and populations. The HARE estimates were imputed in NAM founder's genic haplotypes using gene expression data previously collected in seven diverse tissues [26]. The objectives of the study were to: i) partition gene expression variation into *cis* and *trans* components, ii) impute HARE in NAM and the Goodman Association panels based on the shared NAM founder's haplotypes, iii) assess prediction of many complex traits by using HARE, randomly permuted HARE (preserving haplotype structure only), and measured expression within and across populations, and iv) integrate HARE from different tissues to predict complex phenotypes within and across populations.

Results

Phenotypic and genetic diversity in NAM and Goodman Association panel

The phenotypic distribution of 26 diverse traits is presented in S1 Fig, where the average trait value was higher in 18 traits in NAM than Goodman Association panel. The haplotype frequency was also variable across these two panels (S2 Fig). The median haplotype count across genes (reference regions) was 100 in NAM whereas it was 8 in the Goodman panel. The majority of haplotypes were present in 100 lines as expected from biparental populations with 200 inbred progenies in NAM. Each reference region in NAM was dominated by haplotypes from the common parent (B73), representing half of the haplotypes. We also calculated haplotype entropy from haplotype frequency counts in each reference region to reflect the average information content of haplotypes in reference regions. We observed a higher median entropy of 3.03 in Goodman panel when compared to 2.3 in NAM (S2 Fig).

145 **Variance partition in expression**

146 We hypothesized that the majority of the expression would be contributed by *trans* acting factors
147 as compared to the *cis* component. To test this hypothesis, we fit the model with haplotypes in
148 each gene region as *cis* and the haplotype relationship matrix (HRM) combined across all genes
149 as *trans* (model 1; Fig 1, B). For most of the genes, higher variance in RNA expression was
150 explained by the *trans* component (Fig 2a right) as compared to the *cis* component (Fig 2a left),
151 irrespective of the tissue. Overall, *cis* haplotypes contributed only 34% (31- 38% across
152 individual tissues) of the total genetic variation in expression across all tissues.

153

154 The total heritability was quantified as the proportion of variation contributed by *cis* and *trans*
155 components to the total variation in gene expression. Overall, the gene expression was highly
156 heritable with an average ranging from 50% to 59% across tissues (Fig 2b right). Though the
157 gene expression was highly heritable, the heritability was largely contributed by *trans* compared
158 to *cis* (Fig 2b). The large effect of *trans* could be due to many small-effect molecular
159 connections from *trans* regulators [11,28].

160

161 We analyzed the result separately for a set of genes (~8,000 genes) with higher expression across
162 each tissue to see if the patterns in their expression were any different from other genes. The *cis*
163 haplotype explained a similar amount of variation (median 33%), however, the heritability
164 increased slightly from a median of 54% to 60% across all tissues in a set of highly expressed
165 genes.

166

167 **Transferability of Haplotype Associated RNA expression (HARE)**

168 We used three different models to estimate HARE. Model 1 included both *cis* and *trans* fit as
169 random effects, and model 2 and model 3 included only *cis* fit either as a fixed or random effect.
170 To determine how close the HARE estimates were to measured expression, we estimated their
171 correlations across all tissues. A correlation close to 1 implied that the majority of variation in
172 gene expression was contributed by *cis*, whereas a correlation close to 0 meant most expression
173 was contributed by *trans*. The overall distribution across all expressed genes was similar in all
174 tissues and models with a mean correlation of 0.44 (Fig 3).
175
176 We hypothesized that HARE would include the transferable portion of gene expression based on
177 the underlying haplotype. To test this, we looked at pairwise correlations of HARE from all three
178 models and measured transcript expression across all combinations of genes and tissues.
179 Correlation coefficients ranged from -1 to 1 in all 21 different combinations of 7 diverse tissues
180 (Fig 4, S3 Fig). The median correlation coefficient in measured expression was 0.14 across all
181 tissues, whereas it was 0.4 in HARE. Correlation across tissues was larger for a set of highly
182 expressed genes (~8,000 genes) as compared to the overall set. The median correlation across
183 tissues increased from 0.14 to 0.21 in measured expression and 0.4 to 0.53 in HARE (S5 Fig) in
184 the highly expressed gene set. The HARE imputed from all three models followed similar trends
185 of higher correlation for most of the genes across all tissues as compared to measured transcript
186 expression. Closely related tissues -- for example, mature mid-leaf tissue sampled during midday
187 (LMAD) and midnight (LMAN) were more correlated than other combinations, both in
188 measured expression and HARE (S3 Fig), reflecting the influence of shared gene regulation
189 mechanisms driving these correlations in leaf tissues.
190

191 We looked further into highly correlated genes (correlation > 0.75) and poorly correlated genes
192 (correlation -0.05 to 0.05) across all tissue combinations to see if the large correlations were the
193 result of some very lowly expressed genes. We examined expression in each tissue and filtered
194 values for genes with fragments per million counts <5. In tissue LMAN, out of 10,600 genes
195 with low correlation across tissues, only 3,000 lowly expressed genes were filtered out. Out of
196 11,500 genes with high correlation across tissues, only 1,400 genes showed low expression
197 values across tissues. Therefore, the lowly expressed genes did not drive the higher correlation of
198 HARE estimates across tissues.
199
200 **Genomic prediction using HARE**
201 The high correlation of HARE estimates across tissues suggests that consistent and transferable
202 genetic information is present in HARE. The functional application of HARE was evaluated
203 using genomic prediction within and across populations for 26 agronomically important traits in
204 maize (Table 1). Transferability across populations was evaluated based on prediction accuracy,
205 calculated as the Pearson correlation of observed and predicted trait values. The genomic
206 prediction models were trained to predict traits within and across populations in maize. First, we
207 compared prediction accuracies in three sample traits (days to anthesis, days to silking, and plant
208 height) using HARE estimates and their randomly permuted values ("random HARE",
209 representing only haplotype structure; see Materials and methods), from three different methods
210 (models 1, 2, and 3). We did not see any significant differences in accuracy using any of these
211 imputation methods (S6 Fig), so we used HARE estimates from model 1 (*cis* effects adjusted
212 from *trans* effects) to predict all 26 traits within panel in the Goodman Association panel and
213 across panels in the Goodman Association and NAM.

214

215 **Within-panel prediction using HARE as compared to measured expression or haplotype**
216 **structure (random HARE)**

217 The comparison of prediction accuracy using measured expression and HARE was conducted in
218 the Goodman panel to test the hypothesis that the prediction using HARE would be higher than
219 measured expression. Prediction accuracy by measured expression was highly variable across
220 traits and tissues; in contrast, prediction accuracy by HARE was less variable across tissues. The
221 highest accuracy was observed for flowering time traits (e.g., days to anthesis up to 0.9), using
222 HARE from all tissues, or measured expression from mature mid-leaf tissues (LMAD and
223 LMAN). Overall, HARE resulted in higher prediction accuracy for *all* 26 traits, compared to
224 measured expression in any tissue (Fig 5a and S7 Fig). The highest accuracy increase was for the
225 number of brace roots, which increased from 0.21 to 0.5 using HARE from germinating root (S7
226 Fig). However, the median increase across tissues was highest for trait kernel weight, which
227 increased from 0.2 to 0.5 (Fig 5a). Also, HARE resulted in significantly higher prediction
228 accuracy compared to random HARE for 24 traits (P-value < 0.05) (Fig 5b). Therefore,
229 partitioning expression at the level of gene haplotypes results in higher prediction accuracy,
230 when compared to predictions by measured expression or haplotype structure (random HARE).

231

232 **Cross-panel prediction using HARE as compared to haplotype structure (random HARE)**

233 For all 26 traits and 7 diverse tissues, prediction models were trained using HARE or random
234 HARE across panels in NAM and the Goodman Association to determine if HARE carries
235 functional information beyond haplotype structure. HARE often improved prediction accuracy of
236 many traits when the model was trained in NAM or the Goodman panel as compared to random

237 HARE. HARE significantly increased accuracy by 34.6% and decreased 1.7% across all traits
238 and tissue combinations when the model was trained in NAM (Fig 6a and S1 Table) and only
239 significantly increased by 21.8% when trained in Goodman (Fig 6b and S2 Table). The accuracy
240 was significantly higher in 17 out of 26 traits when trained in NAM and tested in the Goodman
241 panel, *versus* 19 out of 26 traits when trained in Goodman panel and tested in NAM (P-value <
242 0.05). However, the increase in accuracy was highly variable across these two panels. The
243 increase was as high as 15% (for morphological traits: plant height and leaf length) when the
244 model was trained in NAM and tested in the Goodman panel; whereas it was less than 10% when
245 the model was trained in the Goodman panel and tested in NAM (Fig 6a, 6b, and 7). The
246 increase in accuracy over random HARE was also observed when a model was trained only in
247 the sample of 250 NAM RILs (a similar size as the Goodman panel, 10 sample RILs from 25
248 families) to predict 3 traits (Days to anthesis, Days to silking, and Plant height) in Goodman
249 panel (S8 Fig). When the model was trained in NAM the increase in prediction accuracy reached
250 up to 16% over random HARE for the morphological traits, 10% for flowering traits, 8% for
251 yield traits, 12% for kernel composition, and 6% for disease related traits (S1 Table). In general,
252 traits in yield and disease related categories had the lowest accuracy when compared to the traits
253 in other categories. Genomic prediction models using HARE could improve prediction accuracy
254 with simple computational work without any additional cost for data generation. Therefore,
255 haplotype-based models have the potential to improve genomic prediction across populations;
256 however, the improvement depends on the traits of interest. The overall number of significant
257 improvements was higher when using mean or maximum expression, when compared to using
258 the expression of individual tissues, in both directions. Therefore, integrating expression from

259 diverse tissues as mean or maximum expression may contribute to further improvements in
260 prediction accuracy.
261
262 **Discussion**
263 **Cis haplotypes explained one-third of the genetic variation in expression**
264 Consistent with other studies, we found the vast majority of expression to be heritable [28–30].
265 In eQTL mapping, *cis*-eQTL can seem predominant as they are frequently the single largest QTL
266 for a given gene, but this is likely a power and multiple testing issue [12]. By using variance
267 partitioning and assuming a polygenic model, we are likely accurately estimating the relative
268 importance of these two components, *cis* and *trans*.
269 We showed that *cis* haplotype explained around 34% of variation in expression, which given the
270 rapid linkage disequilibrium decay surrounding the gene is still extremely enriched for variance.
271 Similar results were observed by Lemmon et al. [30] in maize and teosinte using hybrid allele
272 specific expression, a complementary technique to our approach. This agree with our molecular
273 knowledge, where, dozens of transcription factors likely regulate each gene [13]. These
274 transcription factors are a result of any regulatory genes modelled as *trans*. In contrast, *cis*
275 variability is a result of variation within or around genes only, empirically lowering the amount
276 of variability explained by a *cis* as compared to the overall *trans* effect as observed in similar
277 experiments in human and yeast [12,29].
278
279 **HARE was highly transferable across tissues as compared to measured transcript**
280 **expression**

281 Variation in gene expression across tissues, developmental stages, genotypes, and experimental
282 conditions has been shown in earlier studies in plants and humans [26,33–35]. Lower
283 correlations in expression for similar genes have been observed across populations in Mogil et al.
284 [36], therefore, high gene expression in one population may not always be as high in diverse
285 panels. The lack of strong correlations in measured transcript expression may result from *trans*
286 effects in the expression, which are specific to tissues, genetic backgrounds, or environmental
287 conditions [11] (S4 Fig). With HARE, we observed higher transferability across tissues as this
288 portion of the variation in gene expression was less sensitive to environmental perturbations and
289 biological contexts. The *cis* regulatory mutations affect expression of fewer genes compared to
290 *trans* effects, so, they result in less pleiotropy and involve fewer functional tradeoffs [37]. In the
291 absence of large pleiotropic effects, selection can act more consistently, so *cis* effects may be
292 more transferable across different backgrounds [37,38].
293
294 HARE can integrate a rich allelic series that is more transferable across different contexts than
295 measured transcript expression which is a result of *cis*, *trans*, their interaction, and environmental
296 effects. Allelic richness is more pronounced in species like maize, which has 20 times higher
297 nucleotide diversity than human beings [39]. Because of high allelic richness in maize, a wide
298 range of possible alleles might lead to the same molecular outcome (for example, gene
299 expression, protein expression, etc.), a concept known as equifinality. Due to equifinality, it has
300 been observed that allelic variants are not always shared across genomes, and transcription is not
301 always correlated with translation [40]. However, the *cis* portion of expression that summarizes
302 allelic richness is highly transferable across tissues. The *cis* variants in HARE located in the
303 close promoter, 5' and 3' untranslated regions, introns and the gene regions are likely consistent

304 across tissues. Further research is needed to understand the effect of enhancer and tissues
305 interaction in the variation on *cis* effects, however the current study suggests that it's not the
306 dominant factor.
307
308 **HARE improved prediction over transcriptome expression**
309 Biological information flows along the central dogma from the genome to transcriptome to
310 proteome to metabolome, and finally to complex phenotypes [41]. For most trait and tissue
311 combinations, transcriptome expression yielded lower prediction accuracy when compared to
312 HARE (Fig 5a and S7 Fig). Furthermore, we observed less variability in prediction accuracy
313 using HARE, which points to the context dependence of RNA expression. HARE owes its
314 consistent advantage in prediction accuracy to functional information that does not include non-
315 genetic sources of variability in RNA expression (interactions among *trans* and *cis* factors and
316 environment). Transcriptome data from mature leaf tissues yielded higher prediction accuracy
317 for most of the phenotypes as compared to the young developing tissues from shoots, roots, or
318 kernels tissue, highlighting the variability in expression regulation across different tissues [26].
319 Therefore, gene expression in different tissues may not capture the same functional information.
320 Most of the phenotypes in this study were measured under field conditions in mature tissues or
321 kernels in different seasons (e.g., flowering traits, agronomic/field traits). Therefore, mature leaf
322 tissue's expression measured in the field should be "closer" to these phenotypes, allowing higher
323 prediction accuracy, compared to expression at the seedling stage measured under controlled
324 conditions. With HARE, the contextual issue was less pronounced resulting in more stable
325 prediction accuracy from any of these tissues.
326

327 **Baseline for comparison of genomic prediction models is important**

328 To determine if haplotype expression carries functional information in addition to haplotype
329 structure in genomic prediction, we used genetic signals produced by random HARE as a
330 baseline for our genomic prediction models. Prior studies have used different baselines to assess
331 genomic prediction models. For example, Westwhues et al. [42] used traditional pedigree BLUP
332 as a baseline for predicting seven complex traits in hybrids as compared to using genomic
333 sequence, metabolomes, transcriptome or a combinations of these; Azodi et al. [2] used the first
334 five principal components in the marker data and compared these with the genomic and
335 transcriptome data to predict three traits; and Li et al. [5] used a genomic BLUP model with SNP
336 data and compared it to extensions with additional endophenotypes in the model to predict nine
337 traits. In this study, randomly permuting the HARE estimates 100 times while preserving
338 haplotype structure, allowed us to assess the accuracy of genomic prediction in the absence of
339 functional information in haplotype values, and to directly test the significance of HARE over
340 haplotype structure. The significantly higher prediction accuracy of HARE affirmed that HARE
341 carried functional information beyond haplotype structure.

342

343 **HARE captured functional information beyond haplotype structure**

344 The benefits of using haplotypes over SNPs, and transcriptomes over SNPs in genomic
345 prediction has been highlighted in earlier studies [4,5,7–10]. Our study here integrated both
346 haplotypes and transcriptome information (as HARE) in the prediction of complex traits.
347 Haplotypes can capture the interaction and epistasis occurring in genic regions, which cannot be
348 captured by SNP data alone [4–6,42]. Another issue in genomic prediction models is
349 overparameterization, where there are more predictors than observations [2,43]. By using

350 transcriptome data rather than SNPs as predictors, the feature dimension can be reduced from
351 millions to thousands, which should make the model more transferable by addressing the curse
352 of dimensionality. This approach could be further improved by functional annotations about gene
353 expression, which could give more or less importance to some genes in HARE, based on prior
354 knowledge about their effect on phenotypes.
355
356 **Tapping into a new source of functional information using HARE**
357 Here, we presented a novel method for imputing HARE using the Practical Haplotype Graph
358 (PHG) and a mixed model approach (Fig 1, 8). Measuring the transcriptome in multiple tissues
359 for every population is expensive, while imputing expression is easier and cost effective. Here
360 we used existing transcriptomes profiled in 7 diverse tissues of the Goodman Association panel
361 consisting of 280 diverse lines to get HARE estimates in NAM founders' haplotypes. HARE
362 estimates were then imputed in the NAM panel consisting of 5000 lines using the PHG. Imputing
363 expression was not only cheaper, it also contributed to more robust genomic predictions. Other
364 methods for predicting expression from genomic sequence were previously reported however
365 these methods are less accurate [15,44]. Compared to these methods, our approach here requires
366 sparse sequencing data only to obtain haplotypes by the PHG and expression in some genotypes.
367 Therefore, it was less computation intensive and more cost-effective than approaches based on
368 deep neural networks applied to complete sequencing data.
369
370 **Conclusion**
371 We showed that by leveraging the diverse high-quality assemblies through a haplotype graph, we
372 can impute *cis* Haplotype Associated RNA Expression in diverse panels. By showing higher

373 transferability across tissues and moderate correlation with measured expression, we have
374 demonstrated that imputing HARE could generate more stable measurements of gene expression
375 across biological contexts. Also, we have demonstrated that HARE estimates could improve
376 genomic prediction for most complex traits in maize over haplotype structure or measured
377 expression. The important consideration in many genomic prediction and transcriptome studies is
378 the cost of generating the genomics and transcriptomics data. Our approach here utilizes sparse
379 sequencing data to obtain haplotypes and impute expression on those haplotypes using the
380 expression measured in some related genotypes.
381 Future experiments could aim at using HARE to predict across species, using gene regulatory
382 networks to provide priors for key genes and trait combinations, refining expression estimates by
383 adding machine learning models that predict expression from DNA sequence, and finally more
384 explicitly modeling tissue by genotype interactions. However, because a substantial proportion
385 of expression is stable across tissues and it can be estimated by variance partitioning, HARE can
386 be applied to successfully improve phenotypic prediction at modest cost.
387

388 **Materials and methods**

389

390 **Phenotypic data**

391 Two maize panels were evaluated for prediction accuracy: the US Nested Association Mapping
392 (NAM) panel and the Goodman Association panel representing the genetic diversity among
393 maize elite inbred lines. The NAM panel was developed from 25 parents crossed to a common
394 parent B73 and selfed to obtain 200 homozygous recombinant inbred lines (RILs) from each
395 cross, as described in McMullen et al. [20] and Gage et al. [21]. The Goodman Association panel

396 represents the global diversity of inbred lines in public maize breeding programs, including ~282
397 genotypes from tropical and temperate regions, sweet corn, and popcorn lines [19]. The 25 NAM
398 founders are part of the Goodman Association panel, so we excluded them from the Goodman
399 Association panel set for cross-panel prediction.
400
401 We evaluated genomic prediction models for 26 traits belonging to different groups: flowering,
402 morphology, yield-related, kernel composition, and disease (Table 1). These traits were chosen
403 from three publications where they were jointly phenotyped in the two panels [22–25].
404 Phenotypic evaluations for these traits were performed in 2006 and 2007 across 11
405 environments, though not all traits were measured in all environments. The field experiments
406 were conducted using an incomplete block alpha lattice design. The phenotypic values were best
407 linear unbiased predictors (BLUPs), details on the phenotypic measurement and BLUP
408 calculation are presented in the respective studies (Table 1).
409
410 **Table 1. Selected traits for genomic prediction**

Category	Traits	Reference
Flowering	Days to silking	[25]
	Days to anthesis	[25]
	Anthesis silking interval	[25]
	Tassel length	[22]
	Tassel primary branches	[22]

Morphology	Plant height	[25]
	Ear height	[25]
	Leaf length	[22]
	Leaf width	[22]
	Leaf angle	[22]
	Nodes below ear	[22]
	Nodes above ear	[22]
	Number of brace roots	[22]
Yield related	Cob diameter	[22]
	Cob length	[22]
	Ear row number	[22]
	Kernel number per row	[22]
	Ear mass	[22]
	Cob mass	[22]
	Kernel wt	[22]
	Test wt	[22]
	Total kernel number	[22]
Kernel composition	Starch	[24]
	Protein	[24]

	Oil	[24]
Disease	Southern leaf blight	[23]

411

412 **PHG database for NAM and Goodman Association panels**

413 Details on the Practical Haplotype Graph (PHG) were described in [27]. In brief, the database
414 consisted of the genomes of 26 NAM parents and one additional stiff stalk inbred B104. The
415 genomes were divided into reference ranges, where the edges of each reference range were
416 defined by gene boundaries in B73 RefGen_v5. A total of 71,354 reference ranges were
417 identified, where half of them were genic regions. The genotyping-by-sequencing (GBS) reads
418 from NAM RILs [45] and the Goodman Association panel [46] were mapped to the PHG
419 database to identify the haplotypes in these populations based on the 27 genomes in the PHG.
420 The SNP calls thus generated were tested for error rate and heterozygosity, imputation accuracy
421 as presented in the original publication [27].

422

423 **Haplotype ID analysis**

424 For each line in the NAM and Goodman panels, a haplotype ID was obtained in each reference
425 region from the PHG database using function pathsForMethod in the rPHG package in R
426 (Bradbury et al., in prep). Since the reference ranges included both genic and intergenic regions,
427 the ranges were filtered to yield only the genic reference ranges based on the B73 RefGen_v5
428 annotations. Shannon entropy of haplotypes counts in the filtered genic reference range were
429 calculated using the R entropy package using the maximum likelihood method [47].

430

431 **Gene expression data**

432 Gene expression data were obtained from Kremling et al. [26]. Details on sampling and
433 expression quantification were presented in the original publication. Seven different tissues
434 (germinating seedlings root: GRoot; germinating seedlings shoot: GShoot; two centimeters from
435 base of leaf 3: L3Base; two centimeters from tip of leaf 3: L3Tip; mature mid-leaf tissue sampled
436 during mid-day: LMAD; mature mid-leaf tissue sampled during mid-night: LMAN; and
437 developing kernels harvested after 350 GDD after pollination: Kern) were included in the
438 analysis. Along with the expression from 7 different tissues, maximum expression and average
439 expression per gene were calculated using a custom script in R.
440
441 The gene expression data from version 3 were obtained in version 5 of the genome by mapping
442 B73 v3 genes to the v5 reference genome. Genes that did not map or mapped in multiple
443 positions were removed from the analysis. The final genic haplotype matrix included ~18,000
444 genes with one-to-one correspondence between the two versions of the genome.
445
446 **Variance partition in gene expression**
447 The variance components in gene expression were estimated using the R package regress and
448 genetic values were obtained by solving mixed model equations by restricted maximum
449 likelihood (REML) [48]. We fit a linear mixed model for each gene to partition variance into the
450 fraction attributable to the genic reference range (haplotypes representing *cis* effects) with and
451 without controlling for *trans* effects. The effects of haplotypes in the genic reference range were
452 fit as fixed or random as described below. The statistical models for variance partition were:
453
454 1. $\mathbf{y} = \mathbf{1}\mu + \mathbf{Z}_{cis}\boldsymbol{\alpha} + \mathbf{e}$ (*cis* fixed effects)

2. $\mathbf{y} = \mathbf{1}\mu + \mathbf{u}_{cis} + \mathbf{e}$ (*cis* random effects)

3. $\mathbf{y} = \mathbf{1}\mu + \mathbf{u}_{cis} + \mathbf{u}_{trans} + \mathbf{e}$ (*cis* + *trans* random effects)

where $\mathbf{y}$ is the RNA expression at a given gene, $\mathbf{Z}_{cis}$ is the design matrix for the gene's *cis* haplotypes, $\boldsymbol{\alpha}$ is the vector of fixed effects of *cis* haplotypes on gene expression, $\mathbf{u}_{cis} \sim N(\mathbf{0}, \mathbf{H}_{cis}\sigma^2_{cis})$ is the vector of *cis* haplotypic effects ($\mathbf{H}_{cis} = \frac{\mathbf{Z}_{cis}\mathbf{Z}^T_{cis}}{tr(\mathbf{Z}_{cis}\mathbf{Z}^T_{cis})/n}$), $\mathbf{u}_{trans} \sim N(\mathbf{0},\ \mathbf{H}_{trans}\sigma^2_{trans})$ is the vector of *trans* haplotypic effects as captured by the design matrix $\mathbf{Z}_{trans}$ for haplotypes at all genes ($\mathbf{H}_{trans} = \frac{\mathbf{Z}_{trans}\mathbf{Z}^T_{trans}}{tr(\mathbf{Z}_{trans}\mathbf{Z}^T_{trans})/n}$), $\mathbf{e} \sim N(\mathbf{0}, \mathbf{I}\sigma^2_e)$ is the vector of errors, n is the number of lines in the panel(s), and *tr* is the trace operator (sum of diagonal elements).

The proportion of variance explained by *cis* and *trans* components was estimated from model 3. The *cis* haplotype variance was estimated as $h^2_{cis} = \frac{\sigma^2_{cis}}{(\sigma^2_{cis} + \sigma^2_{trans} + \sigma^2_e)}$, and *trans* variance was estimated as $h^2_{trans} = \frac{\sigma^2_{trans}}{(\sigma^2_{cis} + \sigma^2_{trans} + \sigma^2_e)}$. The proportion of heritable variance is the total proportion of variance explained by *cis* and *trans* estimated as $\frac{\sigma^2_{cis} + \sigma^2_{trans}}{(\sigma^2_{cis} + \sigma^2_{trans} + \sigma^2_e)}$, and *cis* portion of heritable variance estimated as $\frac{\sigma^2_{cis}}{(\sigma^2_{cis} + \sigma^2_{trans})}$.

Haplotype associated RNA expression (HARE)

The HARE estimates were obtained using the regress package in R and genetic values were obtained by solving mixed model equations by REML [48]. Models 1, 2, and 3 were used to obtain HARE estimates for each haplotype in all genic regions.

474 Expression matrices were generated for genes in the Goodman panel and NAM based on the 27
475 haplotypes from NAM parents and B104. Missing haplotype expression was imputed using mean
476 imputation using a custom script in R. The HARE expression matrix was compared with the
477 measured expression matrix in the Goodman panel by pairwise correlation of genes using the *cor*
478 function in R. Pairwise correlation was calculated between measured expression and HARE
479 estimated across all genes. Similarly, transferability across tissues were assessed by pairwise
480 correlation of genes across all 21 different combinations of 7 tissues for both measured
481 expression and HARE.
482
483 **Genomic prediction model and model performance**
484 The genomic prediction model was fit using ridge regression using the glmnet package in R [55]
485 and the optimal value of the regularization parameter λ was determined by minimum mean
486 squared error in 10-fold cross-validation.
487
488 For a given set of *n* individuals and *p* genes, the following linear model was fit:
489 $$\mathbf{y} = \mathbf{X}\boldsymbol{\beta} + \boldsymbol{\varepsilon}$$
490 Where **y** is a *n*-vector of phenotypic values, **X** is the *n* x *p* matrix of expression values (measured
491 expression or HARE estimates), **β** is the *p*-vector of effects of expression on phenotypes and $\boldsymbol{\varepsilon}$
492 $\sim N(\mathbf{0}, \mathbf{I}\sigma_{\varepsilon}^{2})$ is the vector of errors.
493
494 **Assessment of genomic prediction ability**
495 Part of the signal in genomic prediction by HARE may have been due to the sharing of
496 haplotypes in these populations. Therefore, we established a baseline for genomic prediction by

using random HARE estimates for haplotypes while preserving the haplotype structure (random HARE). For random HARE, the HARE estimates were permuted at the haplotype level, so that each gene had the same HARE estimates, but HARE estimates were randomly matched to haplotypes. For example, if lines 1 and 2 carried the same haplotype at gene *j*, after permutation, both lines got the same random value for imputed expression (Fig 1). The significance of using HARE over random HARE was assessed by using a Monte Carlo procedure with 100 random permutations of HARE [49]. P-values are calculated as $\frac{(r+1)}{(k+1)}$ where $k = 100$ is the total number of permutations and r is the number of permutations with accuracy greater than using HARE (accuracy of random HARE greater than accuracy of HARE).

The prediction accuracy of the genomic prediction models was defined as the Pearson correlation coefficient between the observed trait values ($\mathbf{y}$) and predicted values ($\hat{\mathbf{y}}$) in each of the test sets using the *cor* function in R.

Within-panel prediction

In within-panel prediction, the prediction was carried out only in the Goodman panel using the measured expression, HARE, and random HARE (representing haplotype structure). We used a 5-fold cross-validation procedure for all data sets. The panel was randomly partitioned into 80% training set and 20% testing set. Partitions were repeated 20 times. Pearson correlation was individually calculated in each of the 20 partitions and averaged over partitions to test for significance. For a single trait and tissue combination, the model was run for 2000 times for random HARE and 20 times for HARE and measured expression.

520 **Cross-panel prediction**

521 For cross-population prediction, the model was either trained in NAM and tested in the
522 Goodman panel or vice versa for all traits. The 25 NAM founders are part of the Goodman
523 Association panel, so we excluded them from the Goodman Association panel set for cross-panel
524 prediction. To account for sample size differences (5000 in NAM *versus* 250 in the Goodman
525 panel), 20 random subsets of NAM equivalent to the size of Goodman panel were created, taking
526 10 RILs from each family. The model was trained in the 20 random subsets of NAM RILs and
527 predicted in the Goodman panel and vice versa for three sample traits: Days to anthesis (DTA),
528 Days to silking (DTS), and Plant height (PH). The prediction accuracy was averaged across 20
529 random subsets.

530

531 **Acknowledgments**

532 This study was conducted using the gene expression data collected in seven tissues of Goodman
533 Association Panel (Kremling et al. [26]) and the Practical Haplotype Graph database for the
534 Goodman Association Panel and Nested Association Mapping Panel (Valdes Franco et al. [27]).
535 We thank Sara Miller for copy editing.

536

537

538 **References**

539 1. Meuwissen THE, Hayes BJ, Goddard ME. Prediction of total genetic value using genome-wide dense
540 marker maps. Genetics. 2001;157: 1819–1829.

541 2. Azodi CB, Pardo J, VanBuren R, de los Campos G, Shiu S-H. Transcriptome-Based Prediction of
542 Complex Traits in Maize. Plant Cell. 2020;32: 139–151. doi:10.1105/tpc.19.00332

543 3. Xu Y, Xu C, Xu S. Prediction and association mapping of agronomic traits in maize using multiple
544 omic data. Heredity. 2017;119: 174–184. doi:10.1038/hdy.2017.27

545 4. Guo Z, Magwire MM, Basten CJ, Xu Z, Wang D. Evaluation of the utility of gene expression and
546 metabolic information for genomic prediction in maize. Theor Appl Genet. 2016;129: 2413–2427.
547 doi:10.1007/s00122-016-2780-5

548 5. Li Z, Gao N, Martini JWR, Simianer H. Integrating Gene Expression Data Into Genomic Prediction.
549 Front Genet. 2019;10. doi:10.3389/fgene.2019.00126

550 6. Schrag TA, Westhues M, Schipprack W, Seifert F, Thiemann A, Scholten S, et al. Beyond Genomic
551 Prediction: Combining Different Types of *omics* Data Can Improve Prediction of Hybrid
552 Performance in Maize. Genetics. 2018;208: 1373–1385. doi:10.1534/genetics.117.300374

553 7. Hayes BJ, Chamberlain AJ, McPARTLAN H, Macleod I, Sethuraman L, Goddard ME. Accuracy of
554 marker-assisted selection with single markers and marker haplotypes in cattle. Genet Res. 2007;89:
555 215–220. doi:10.1017/S0016672307008865

556 8. Hess M, Druet T, Hess A, Garrick D. Fixed-length haplotypes can improve genomic prediction
557 accuracy in an admixed dairy cattle population. Genet Sel Evol. 2017;49: 54. doi:10.1186/s12711-
558 017-0329-y

559 9. Won S, Park J-E, Son J-H, Lee S-H, Park BH, Park M, et al. Genomic Prediction Accuracy Using
560 Haplotypes Defined by Size and Hierarchical Clustering Based on Linkage Disequilibrium. Front
561 Genet. 2020;11. doi:10.3389/fgene.2020.00134

562 10. Schopp P, Müller D, Technow F, Melchinger AE. Accuracy of Genomic Prediction in Synthetic
563 Populations Depending on the Number of Parents, Relatedness, and Ancestral Linkage
564 Disequilibrium. Genetics. 2017;205: 441–454. doi:10.1534/genetics.116.193243

565 11. Signor SA, Nuzhdin SV. The Evolution of Gene Expression in cis and trans. Trends Genet. 2018;34:
566 532–544. doi:10.1016/j.tig.2018.03.007

567 12. Albert FW, Bloom JS, Siegel J, Day L, Kruglyak L. Genetics of trans-regulatory variation in gene
568 expression. eLife. 2018;7: 7:e3547. doi:10.7554/eLife.35471

569 13. Tu X, Mejía-Guerra MK, Valdes Franco JA, Tzeng D, Chu P-Y, Shen W, et al. Reconstructing the
570 maize leaf regulatory network using ChIP-seq data of 104 transcription factors. Nat Commun.
571 2020;11: 5089. doi:10.1038/s41467-020-18832-8

572 14. Wittkopp PJ, Haerum BK, Clark AG. Evolutionary changes in cis and trans gene regulation. Nature.
573 2004;430: 85–88. doi:10.1038/nature02698

574 15. Washburn JD, Mejia-Guerra MK, Ramstein G, Kremling KA, Valluru R, Buckler ES, et al.
575 Evolutionarily informed deep learning methods for predicting relative transcript abundance from
576 DNA sequence. Proc Natl Acad Sci. 2019;116: 5542–5549. doi:10.1073/pnas.1814551116

577 16. Grundberg E, Adoue V, Kwan T, Ge B, Duan QL, Lam KCL, et al. Global Analysis of the Impact of
578 Environmental Perturbation on cis-Regulation of Gene Expression. Gibson G, editor. PLoS Genet.
579 2011;7: e1001279. doi:10.1371/journal.pgen.1001279

580 17. Schnable PS, Ware D, Fulton RS, Stein JC, Wei F, Pasternak S, et al. The B73 maize genome:
581 complexity, diversity, and dynamics. Science. 2009;326: 1112–1115. doi:10.1126/science.1178534

582 18. Wallace JG, Bradbury PJ, Zhang N, Gibon Y, Stitt M, Buckler ES. Association Mapping across
583 Numerous Traits Reveals Patterns of Functional Variation in Maize. PLOS Genet. 2014;10:
584 e1004845. doi:10.1371/journal.pgen.1004845

585 19. Flint-Garcia SA, Thuillet A-C, Yu J, Pressoir G, Romero SM, Mitchell SE, et al. Maize association
586 population: a high-resolution platform for quantitative trait locus dissection: High-resolution maize
587 association population. Plant J. 2005;44: 1054–1064. doi:10.1111/j.1365-313X.2005.02591.x

588 20. McMullen MD, Kresovich S, Villeda HS, Bradbury P, Li H, Sun Q, et al. Genetic Properties of the
589 Maize Nested Association Mapping Population. Science. 2009;325: 737–740.
590 doi:10.1126/science.1174320

591 21. Gage JL, Monier B, Giri A, Buckler ES. Ten Years of the Maize Nested Association Mapping
592 Population: Impact, Limitations, and Future Directions. Plant Cell. 2020;32: 2083–2093.
593 doi:10.1105/tpc.19.00951

594 22. Hung H-Y, Shannon LM, Tian F, Bradbury PJ, Chen C, Flint-Garcia SA, et al. ZmCCT and the
595 genetic basis of day-length adaptation underlying the postdomestication spread of maize. Proc Natl
596 Acad Sci. 2012;109: E1913–E1921. doi:10.1073/pnas.1203189109

597 23. Kump KL, Bradbury PJ, Wisser RJ, Buckler ES, Belcher AR, Oropeza-Rosas MA, et al. Genome-
598 wide association study of quantitative resistance to southern leaf blight in the maize nested
599 association mapping population. Nat Genet. 2011;43: 163–168. doi:10.1038/ng.747

600 24. Cook JP, McMullen MD, Holland JB, Tian F, Bradbury P, Ross-Ibarra J, et al. Genetic Architecture
601 of Maize Kernel Composition in the Nested Association Mapping and Inbred Association Panels.
602 PLANT Physiol. 2012;158: 824–834. doi:10.1104/pp.111.185033

603 25. Peiffer JA, Romay MC, Gore MA, Flint-Garcia SA, Zhang Z, Millard MJ, et al. The Genetic
604 Architecture Of Maize Height. Genetics. 2014;196: 1337–1356. doi:10.1534/genetics.113.159152

605 26. Kremling KAG, Chen S-Y, Su M-H, Lepak NK, Romay MC, Swarts KL, et al. Dysregulation of
606 expression correlates with rare-allele burden and fitness loss in maize. Nature. 2018;555: 520–523.
607 doi:10.1038/nature25966

608 27. Franco JAV, Gage JL, Bradbury PJ, Johnson LC, Miller ZR, Buckler ES, et al. A Maize Practical
609 Haplotype Graph Leverages Diverse NAM Assemblies. Genomics; 2020 Aug.
610 doi:10.1101/2020.08.31.268425

611 28. Liu X, Li YI, Pritchard JK. Trans Effects on Gene Expression Can Drive Omnigenic Inheritance.
612 Cell. 2019;177: 1022-1034.e6. doi:10.1016/j.cell.2019.04.014

613 29. GTEx Consortium. Genetic effects on gene expression across human tissues. Nature. 2017;550: 204–
614 213. doi:10.1038/nature24277

615 30. Lemmon ZH, Bukowski R, Sun Q, Doebley JF. The Role of cis Regulatory Evolution in Maize
616 Domestication. Fraser H, editor. PLoS Genet. 2014;10: e1004745. doi:10.1371/journal.pgen.1004745

617 31. Lopez-Arboleda WA, Reinert S, Nordborg M, Korte A. Global genetic heterogeneity in adaptive
618 traits. Evolutionary Biology; 2021 Feb. doi:10.1101/2021.02.26.433043

619 32. Gibson G. Rare and common variants: twenty arguments. Nat Rev Genet. 2012;13: 135–145.
620 doi:10.1038/nrg3118

621 33. Schmid M, Davison TS, Henz SR, Pape UJ, Demar M, Vingron M, et al. A gene expression map of
622 Arabidopsis thaliana development. Nat Genet. 2005;37: 501–506. doi:10.1038/ng1543

623 34. Sekhon RS, Lin H, Childs KL, Hansey CN, Buell CR, Leon N de, et al. Genome-wide atlas of
624 transcription during maize development. Plant J. 2011;66: 553–563. doi:10.1111/j.1365-
625 313X.2011.04527.x

626 35. Melé M, Ferreira PG, Reverter F, DeLuca DS, Monlong J, Sammeth M, et al. The human
627 transcriptome across tissues and individuals. Science. 2015;348: 660–665.
628 doi:10.1126/science.aaa0355

629 36. Mogil LS, Andaleon A, Badalamenti A, Dickinson SP, Guo X, Rotter JI, et al. Genetic architecture of
630 gene expression traits across diverse populations. Epstein MP, editor. PLOS Genet. 2018;14:
631 e1007586. doi:10.1371/journal.pgen.1007586

632 37. Stern DL. Perspective: Evolutionary Developmental Biology and the Problem of Variation.
633 Evolution. 2000;54: 1079–1091. doi:https://doi.org/10.1111/j.0014-3820.2000.tb00544.x

634 38. Wray GA. The evolutionary significance of cis -regulatory mutations. Nat Rev Genet. 2007;8: 206–
635 216. doi:10.1038/nrg2063

636 39. Initial sequence of the chimpanzee genome and comparison with the human genome. Nature.
637 2005;437: 69–87. doi:10.1038/nature04072

638 40. Missra A, Ernest B, Lohoff T, Jia Q, Satterlee J, Ke K, et al. The Circadian Clock Modulates Global
639 Daily Cycles of mRNA Ribosome Loading. Plant Cell. 2015;27: 2582–2599.
640 doi:10.1105/tpc.15.00546

641 41. Fiévet JB, Dillmann C, de Vienne D. Systemic properties of metabolic networks lead to an epistasis-
642 based model for heterosis. Theor Appl Genet. 2009;120: 463. doi:10.1007/s00122-009-1203-2

643 42. Westhues M, Schrag TA, Heuer C, Thaller G, Utz HF, Schipprack W, et al. Omics-based hybrid
644 prediction in maize. Theor Appl Genet. 2017;130: 1927–1939. doi:10.1007/s00122-017-2934-0

645 43. Ramstein GP, Jensen SE, Buckler ES. Breaking the curse of dimensionality to identify causal variants
646 in Breeding 4. Theor Appl Genet. 2019;132: 559–567. doi:10.1007/s00122-018-3267-3

647 44. Zhou J, Theesfeld CL, Yao K, Chen KM, Wong AK, Troyanskaya OG. Deep learning sequence-
648 based ab initio prediction of variant effects on expression and disease risk. Nat Genet. 2018;50:
649 1171–1179. doi:10.1038/s41588-018-0160-6

650 45. Rodgers-Melnick E, Bradbury PJ, Elshire RJ, Glaubitz JC, Acharya CB, Mitchell SE, et al.
651 Recombination in diverse maize is stable, predictable, and associated with genetic load. Proc Natl
652 Acad Sci. 2015;112: 3823–3828. doi:10.1073/pnas.1413864112

653 46. Romay MC, Millard MJ, Glaubitz JC, Peiffer JA, Swarts KL, Casstevens TM, et al. Comprehensive
654 genotyping of the USA national maize inbred seed bank. Genome Biol. 2013;14: R55.
655 doi:10.1186/gb-2013-14-6-r55

656 47. Hausser J, Strimmer K, Strimmer M. Package "Entropy." 2012.

657 48. Clifford D, McCullagh P. The regress function. R news. 6th ed. : 6–10.

658 49. North BV, Curtis D, Sham PC. A Note on the Calculation of Empirical P Values from Monte Carlo
659 Procedures. Am J Hum Genet. 2002;71: 439–441.

660

661 S1 Fig. Phenotypic distribution of 26 traits in NAM and the Goodman Association panel

662

663 S2 Fig. a. Haplotype counts distribution in the Goodman association panel (left) and NAM panel
664 (right) across all genic reference ranges. b. Haplotype entropy in Goodman (left) and NAM
665 (right) panel in each reference range. Median haplotype counts were 8 and 100 in the Goodman
666 panel and NAM, respectively, resulting in higher entropy in the Goodman panel as compared to
667 NAM. Entropy was calculated from haplotype counts in each reference region.

668

669 S3 Fig. Correlation distribution of expression between tissues. The four panels represent HARE
670 estimates from models 1 (*cis* only fixed), 2 (*cis* only random), and 3 (*cis* random while
671 accounting for *trans*), as well as measured expression. The different color lines in each panel
672 represent 21 different combinations of the 7 different tissues as labeled on the right: germinating
673 seedlings root (GRoot), germinating seedlings shoot (GShoot), two cm from base of leaf 3
674 (L3Base), two cm from tip of leaf 3 (L3Tip), mature mid-leaf tissue sampled during mid-day
675 (LMAD), mature mid-leaf tissue sampled during mid-night (LMAN), and developing kernels
676 harvested after 350 growing degree days after pollination (Kern). The imputed expression from
677 models was highly correlated between tissues when compared to the measured transcript
678 expression. In all panels, closely related tissues like matured mid-leaf tissue expression sampled
679 during mid-day (LMAD) and matured mid-leaf tissue expression sampled during mid-night
680 (LMAD) were highly correlated.

681

682 S4 Fig. Correlation distribution of *trans* components of expression between tissues. The different
683 color lines in each panel represent 21 different combinations of the 7 different tissues as labeled

684 on the right: germinating seedlings root (GRoot), germinating seedlings shoot (GShoot), two cm
685 from base of leaf 3 (L3Base), two cm from tip of leaf 3 (L3Tip), mature mid-leaf tissue sampled
686 during mid-day (LMAD), mature mid-leaf tissue sampled during mid-night (LMAN), and
687 developing kernels harvested after 350 growing degree days after pollination (Kern). Similar to
688 measured transcript expression, closely related tissues like matured leaf expression during the
689 day (LMAD) and matured leaf expression during the night (LMAD) were highly correlated.
690
691 S5 Fig. Haplotype associated RNA expression (HARE) was highly correlated across tissues as
692 compared to measured transcript expression. Different colors represent HARE imputed from
693 three statistical models: Model 1 (*cis* fixed effect), 2 (*cis* random effect), and 3 (*cis* + *trans*
694 random effects), and measured transcript expression. The distribution is the pairwise correlation
695 of ~8000 highly expressed genes across 21 different combinations from 7 different tissues.
696
697 S6 Fig. Prediction accuracy using HARE from model 1, 2, and 3 (see methods) for predicting
698 three different traits: Days to Anthesis (DTA), Days to Silking (DTS), and Plant Height (PH)
699 using a) model trained in NAM and tested in Goodman b) model trained in Goodman and tested
700 in NAM. The different symbols represent HARE from different tissues: germinating seedlings
701 shoot (GShoot), developing kernels harvested after 350 growing degree days after pollination
702 (Kern), 2 cm from base of leaf 3 (L3Base), and mature mid-leaf tissue sampled during mid-day
703 (LMAD).
704
705 S7 Fig. Within-panel prediction accuracy in the Goodman panel using HARE (red dot), 100
706 random HARE (box plot), and measured expression (blue dot) from individual tissues or all

707 tissues integrated as mean or maximum expression. Individual tissues included: germinating
708 seedlings root (GRoot), germinating seedlings shoot (GShoot), two cm from base of leaf 3
709 (L3Base), two cm from tip of leaf 3 (L3Tip), mature mid-leaf tissue sampled during mid-day
710 (LMAD), mature mid-leaf tissue sampled during mid-night (LMAN), and developing kernels
711 harvested after 350 growing degree days after pollination (Kern). The model was trained in 80%
712 of the panel and tested in the remaining 20%.
713
714 S8 Fig. Change in prediction accuracy using HARE over the mean of random expression (blue
715 dashed line) from five different tissues: germinating seedlings root (GRoot), two cm from base
716 of leaf 3 (L3Base), mature mid-leaf tissue sampled during mid-day (LMAD), mature mid-leaf
717 tissue sampled during mid-night (LMAN), and developing kernels harvested after 350 growing
718 degree days after pollination (Kern). Genomic prediction models were (a) trained in the
719 Goodman panel and tested in 20 subsets of NAM, (b) trained in 20 subsets of NAM and tested in
720 the Goodman panel. The subsets of NAM were generated by randomly selecting 10 genotypes
721 from each family resulting in a total of 250 genotypes (see methods). Accuracy was averaged
722 over the 20 random subsets before determining significance. The black shapes represent
723 statistically significant differences at P-values <0.05 and red shapes represent no statistical
724 significance. P-values were calculated using a Monte Carlo procedure.
725
726 S1 Table. Prediction accuracy of 26 complex traits in the Goodman Association panel using
727 HARE from seven diverse tissues: germinating seedlings root (GRoot), germinating seedlings
728 shoot (GShoot), 2 cm from base of leaf 3 (L3Base), two cm from tip of leaf 3 (L3Tip), mature
729 mid-leaf tissue sampled during mid-day (LMAD), mature mid-leaf tissue sampled during mid-

night (LMAN), and developing kernels harvested after 350 growing degree days after pollination (Kern), mean, and maximum expression of genes across all tissues. P value (high) and P value (low) were calculated using a Monte Carlo procedure to test if the accuracy using HARE was significantly higher or lower than random HARE. Models were trained in NAM and tested in Goodman Association panel.

S2 Table. Prediction accuracy of 26 complex traits in NAM using HARE from 7 diverse tissues: germinating seedlings root (GRoot), germinating seedlings shoot (GShoot), 2 cm from base of leaf 3 (L3Base), 2 cm from tip of leaf 3 (L3Tip), mature mid-leaf tissue sampled during mid-day (LMAD), mature mid-leaf tissue sampled during mid-night (LMAN), and developing kernels harvested after 350 growing degree days after pollination (Kern), mean, and maximum expression of genes across all tissues. P value (high) and P value (low) were calculated using a Monte Carlo procedure to test if the accuracy using HARE was significantly higher or lower than random HARE. Models were trained in Goodman Association panel and tested in NAM.

List of Figures:

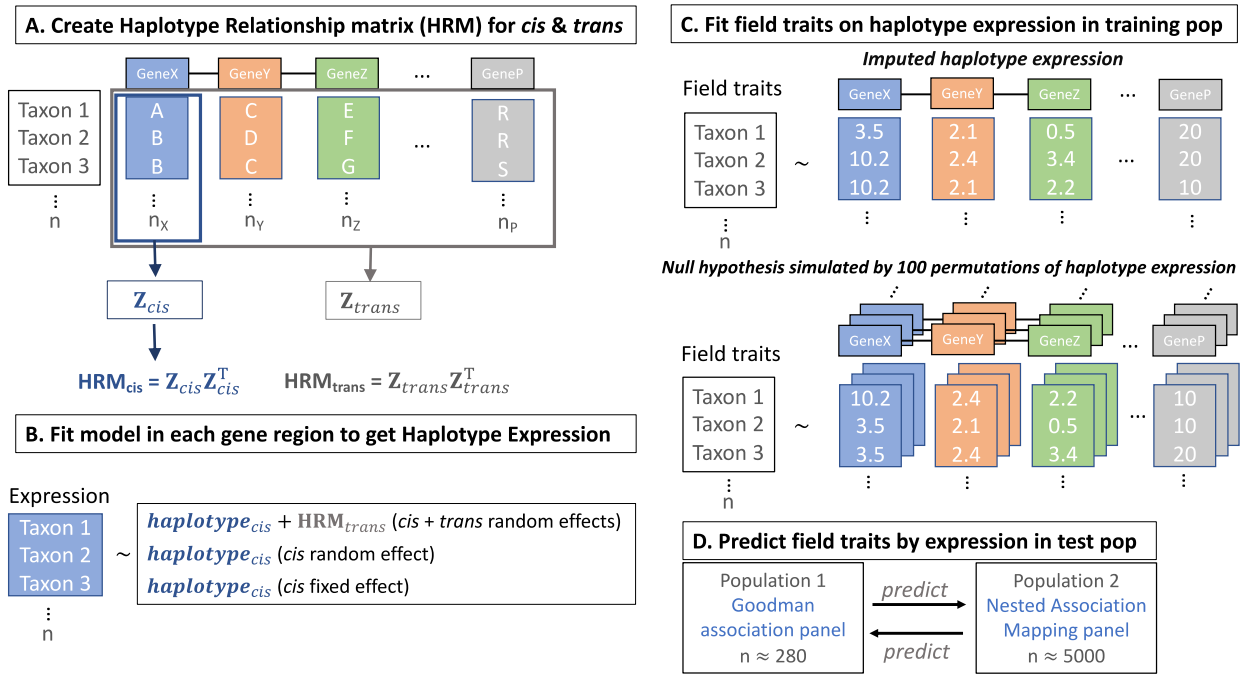

Fig 1. Experimental methods on calculating haplotype associated RNA expression (HARE) and using HARE values to predict complex traits. A. The haplotypes of 26 NAM founders and one additional stiff stalk inbred line were identified in each gene region of the Goodman Association panel by mapping GBS reads (presented in detail in Valdes Franco et al. [27]) to the indexed pangenome of 27 lines. Haplotype relationship matrices (HRM_{cis}) were created in each gene region and all genic HRM_{cis} were combined to get HRM_{trans} to control for *trans* effects, B. Using gene expression from seven tissues [26], fixed or random effects models were fitted in each gene region with or without controlling for *trans* effects for each gene, C. Models were trained using field phenotypes in the Goodman panel or the NAM panel using HARE estimates or 100 randomly permuted HARE values while preserving haplotype structure, and D. Trained models were used to predict complex traits across populations.

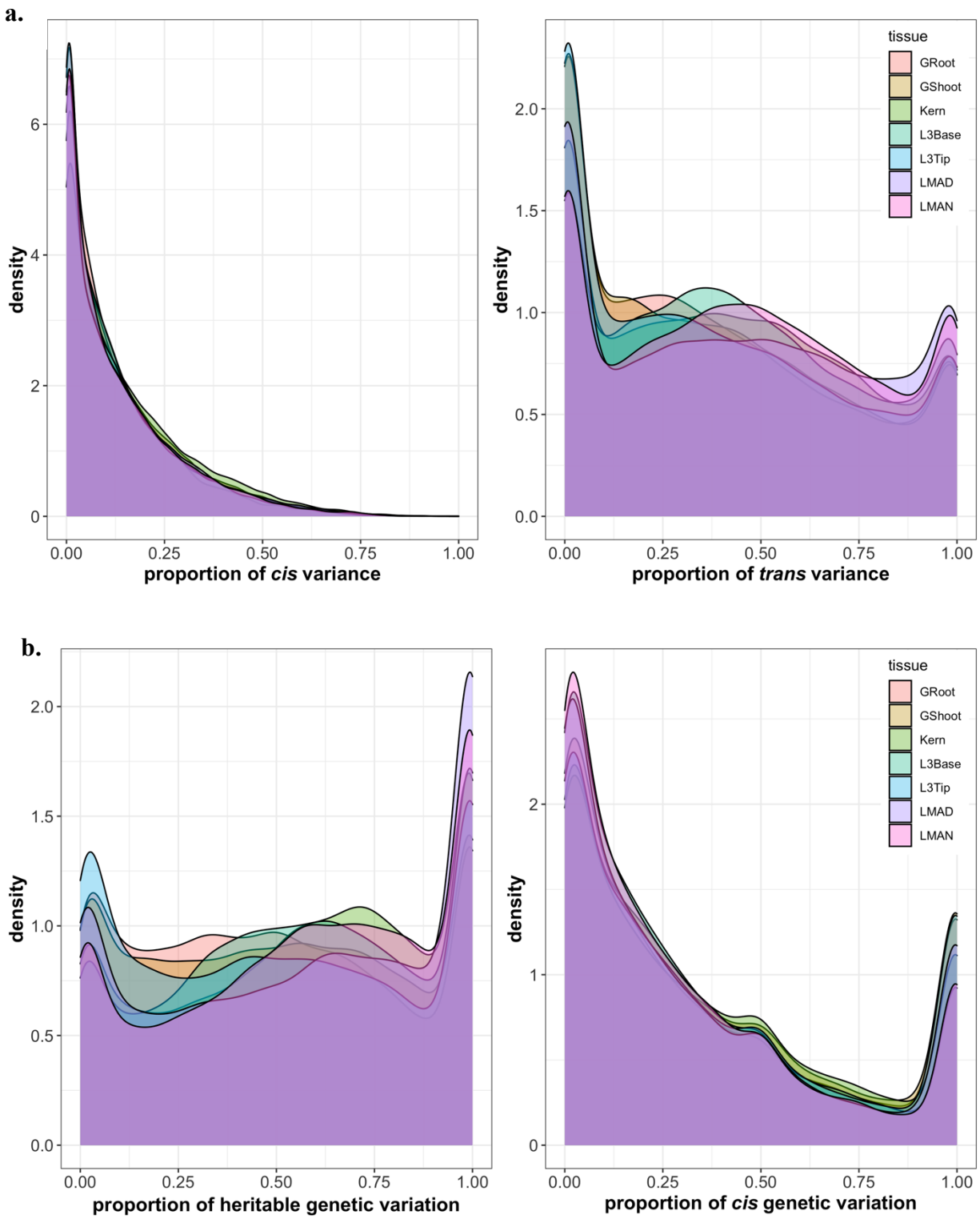

Fig 2. *Cis* haplotype explained one-third of the total genetic variance in expression. a. Proportion of variation explained by *cis* (left) and *trans* (right) components, b. Proportion of

763 heritable genetic variation over phenotypic variation (left) and proportion of heritable genetic
764 variation explained by *cis* (right) in gene expression across seven different tissues. Heritable
765 variation was calculated in each gene as the ratio of the sum of *cis* and *trans* variance to total
766 variance. Different colors represent seven diverse tissues in maize: germinating seedlings root
767 (GRoot), germinating seedlings shoot (GShoot), two cm from base of leaf 3 (L3Base), two cm
768 from tip of leaf 3 (L3Tip), mature mid-leaf tissue sampled during mid-day (LMAD), mature mid-
769 leaf tissue sampled during mid-night (LMAN), and developing kernels harvested after 350
770 growing degree days after pollination (Kern).
771

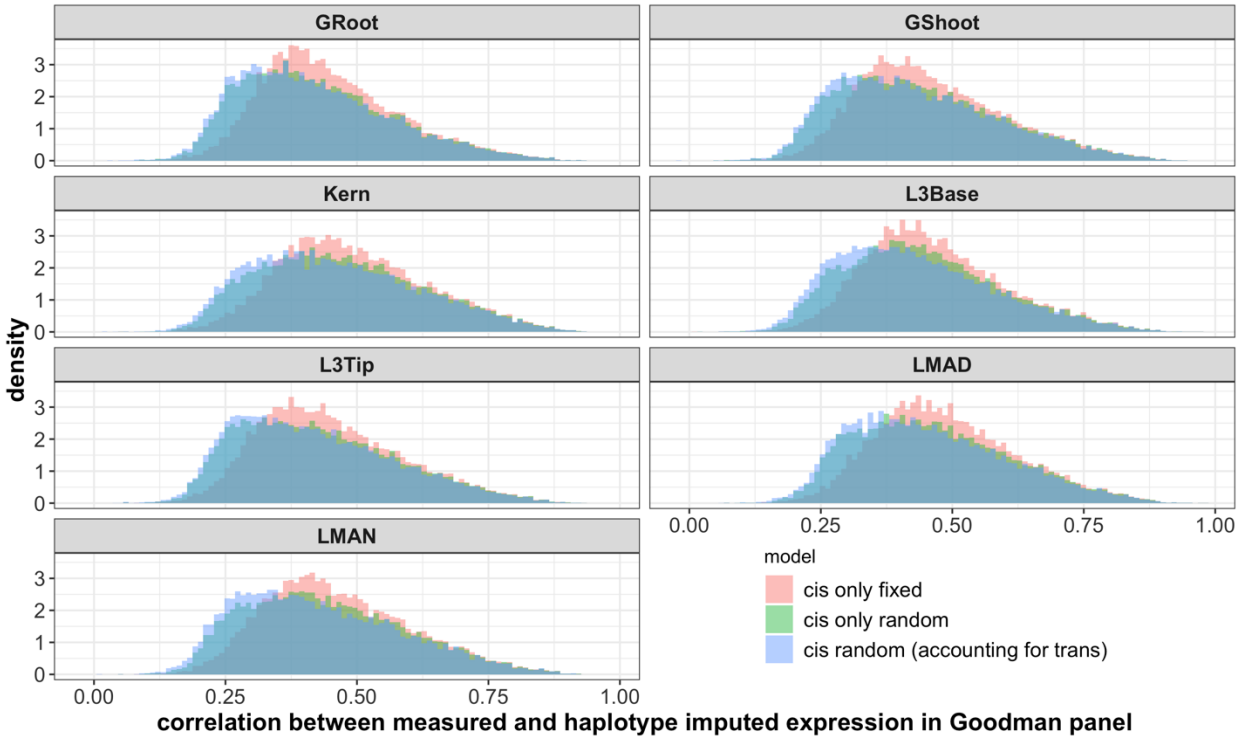

772

773 **Fig 3. Haplotype associated RNA expression (HARE) was moderately correlated with**
774 **measured RNA expression across seven diverse tissues.** The different colors represent HARE
775 imputed from three statistical models: Model 1 (*cis* fixed effect), 2 (*cis* random effect), and 3 (*cis*

776 + *trans* random effects). Transcripts from measured RNA expression was a result of genetic

777 signals in both *trans* and *cis*. Therefore, the correlation was moderate for most of the genes.

778

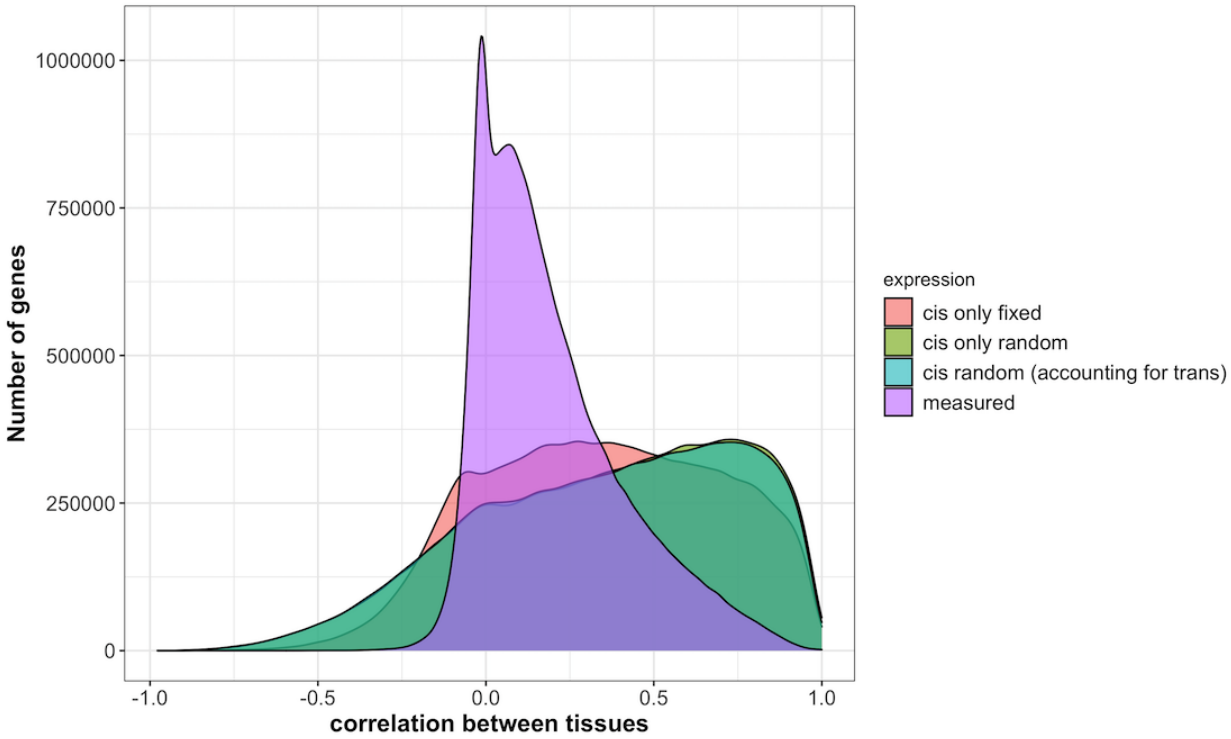

779

780 **Fig 4. Haplotype associated RNA expression (HARE) was highly correlated across tissues**

781 **as compared to measured transcript expression.** Different colors represent HARE imputed

782 from 3 statistical models: Model 1 (*cis* fixed effect), 2 (*cis* random effect), and 3 (*cis* + *trans*

783 random effects), and measured transcript expression. The distribution is pairwise correlation of

784 genes across 21 different combinations from 7 different tissues.

785

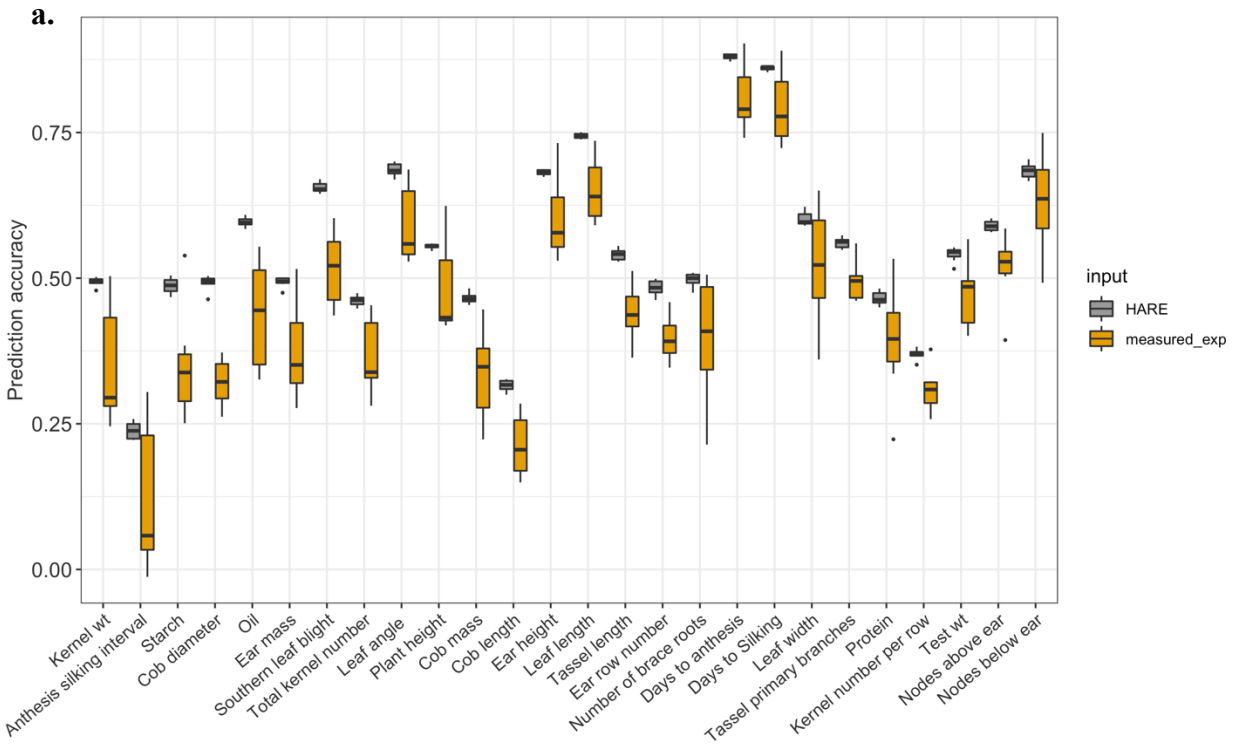

786

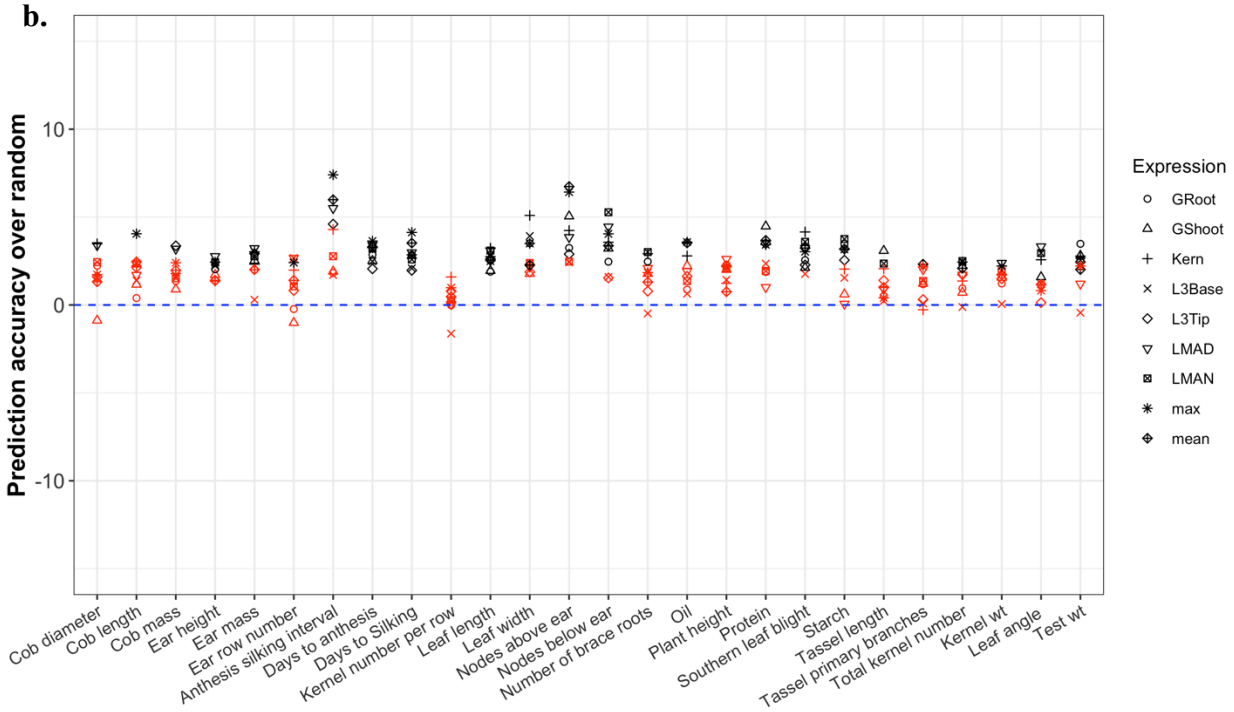

787

788 **Fig 5. HARE improved within-panel prediction accuracy over measured expression and**

789 **random HARE for most of the traits.** (a) Prediction accuracy within the Goodman Association

790 panel using HARE and measured expression (measured_exp) from all tissues arranged by

prediction differential. (b) Change in prediction accuracy using HARE over the mean accuracy from random HARE (blue dashed line). Different symbols represent HARE from different tissues. The black shapes represent statistically significant differences at P-value <0.05 and red shapes are without significant differences. P-values calculated using Monte Carlo procedure.

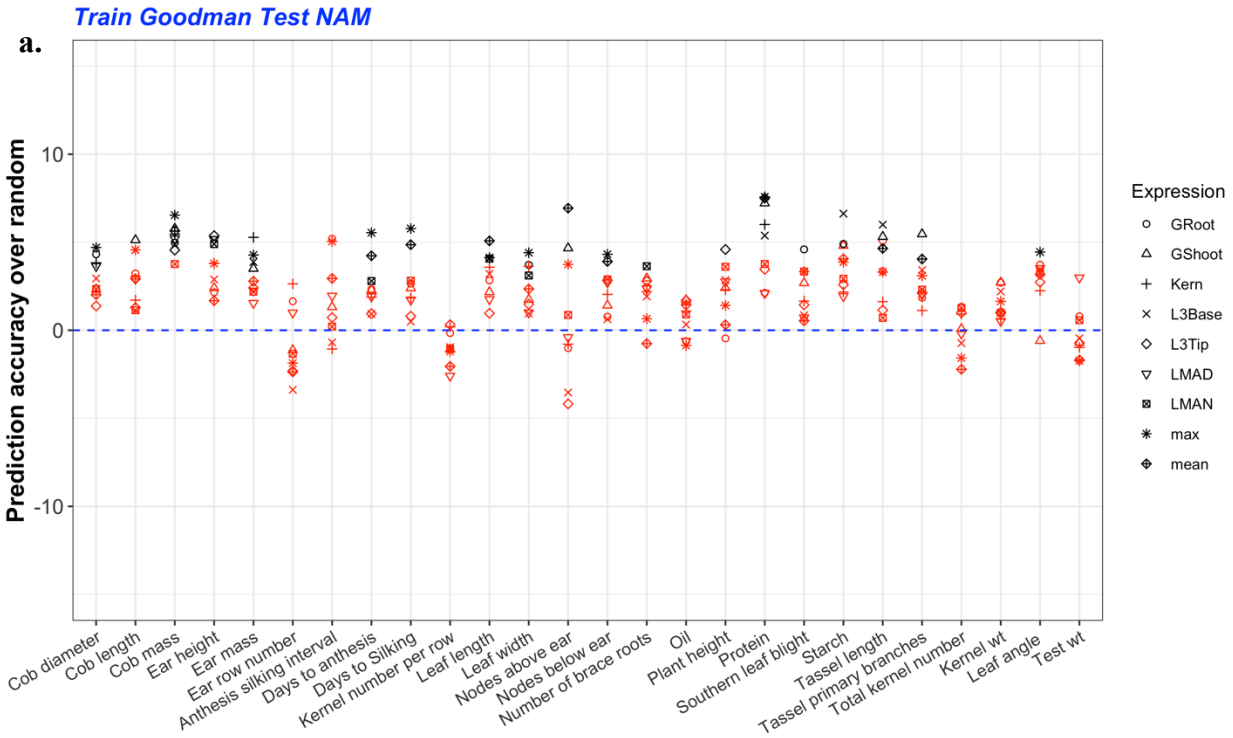

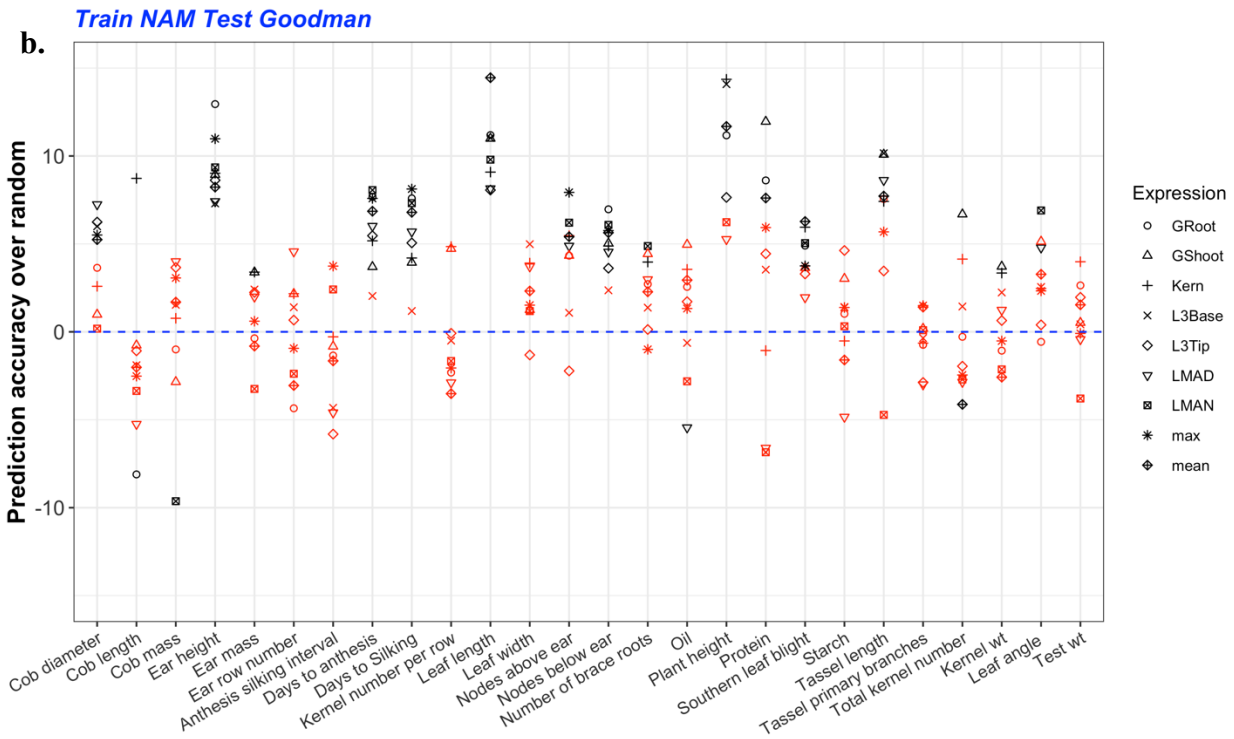

Fig 6. HARE improved cross-panel prediction accuracy over random expression values for most of the traits. Change in prediction accuracy using HARE over the mean accuracy from random HARE (blue dashed line) for models (a) trained in the Goodman panel and tested in NAM, (b) trained in NAM and tested in the Goodman panel. The different symbols represent HARE from different tissues: germinating seedlings root (GRoot), germinating seedlings shoot (GShoot), two cm from base of leaf 3 (L3Base), two cm from tip of leaf 3 (L3Tip), mature mid-leaf tissue sampled during mid-day (LMAD), mature mid-leaf tissue sampled during mid-night (LMAN), and developing kernels harvested after 350 growing degree days after pollination (Kern). The black shapes represent statistically significant differences at P-values <0.05 and red shapes represent no statistical significance. P-values were calculated using a Monte Carlo procedure.

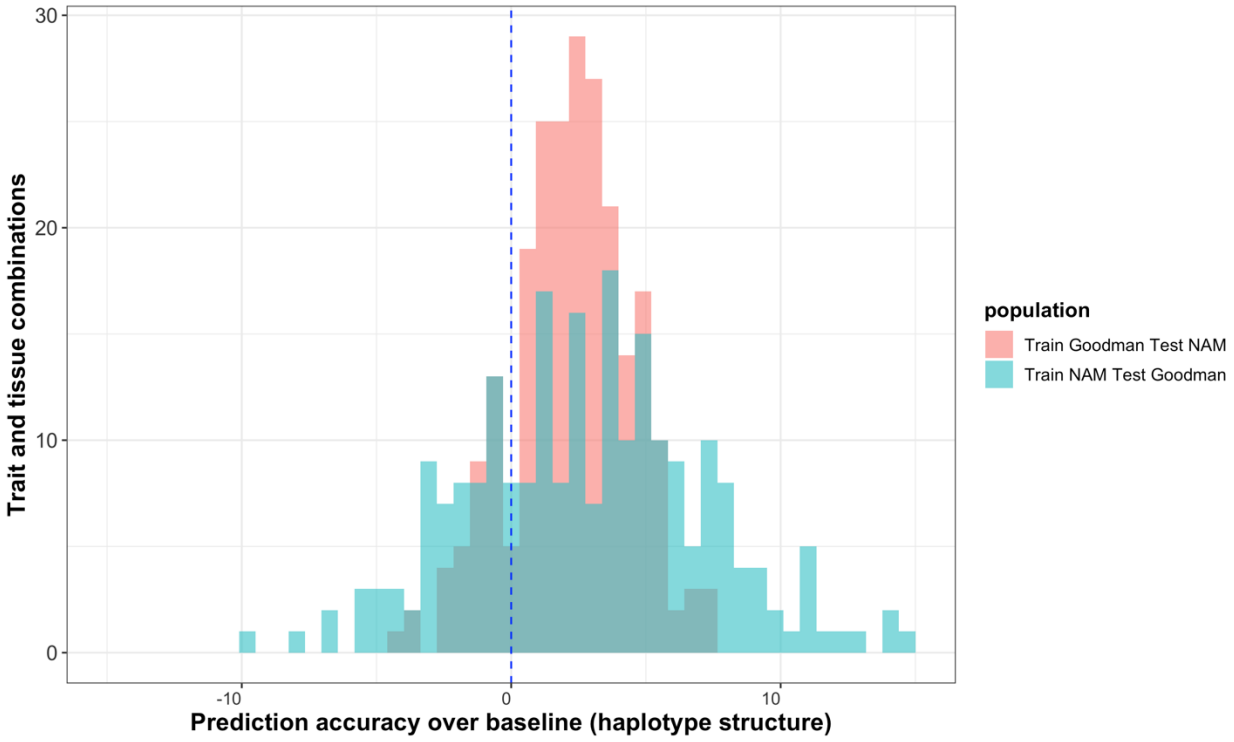

Fig 7. HARE increased prediction accuracy by up to 14% when the model was trained in NAM and tested in the Goodman panel. Summarized differences in prediction accuracy using HARE over the mean accuracy from random HARE (representing haplotype structure) across 26 phenotypes and 7 diverse tissues. The blue dashed line is the mean of the average prediction accuracy using random HARE across each trait and tissue combination.

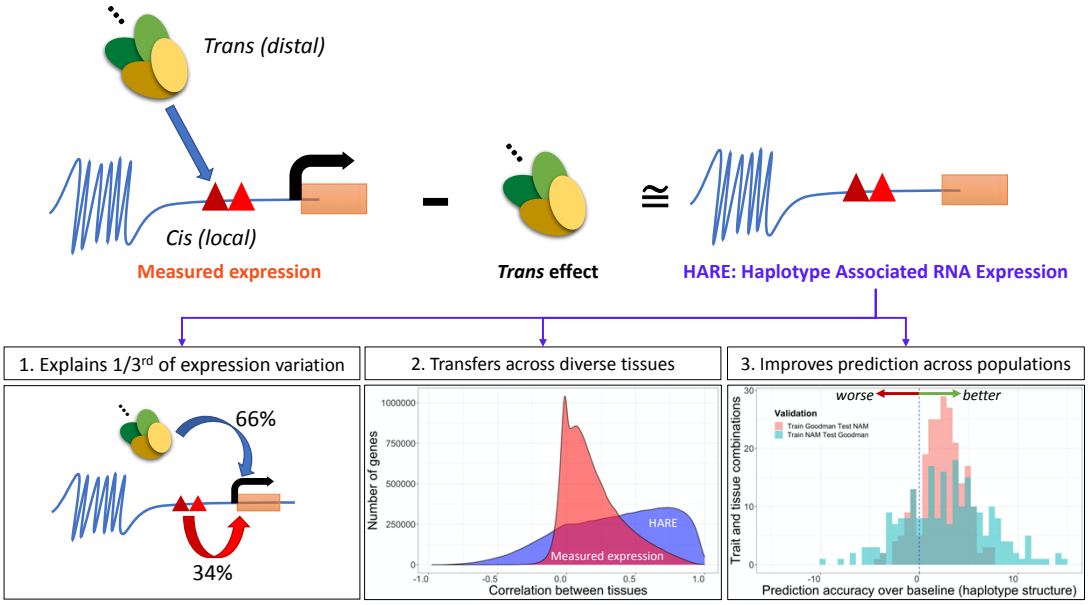

Fig 8. Graphical Summary of the Study. *Cis* haplotype associated RNA expression (HARE) was obtained from subtracting *trans* effects from measured expression. 1. The *cis* haplotypes explained one-third of the variation in expression. 2. The HARE estimates were highly transferrable across tissues compared to measured expression. 3. HARE improved prediction within and across populations in maize.